in silico Plants, 2023, **5**, 1–15
https://doi.org/10.1093/insilicoplants/diad003
Advance access publication 19 February 2023
Original Research

in silico Plants

OXFORD

Original Research

A mathematical model integrates diverging PXY and MP interactions in cambium development

Kristine S. Bagdassarian[1], J. Peter Etchells[1], and Natasha S. Savage[*2]

[1]Department of Biosciences, Durham University, South Road, DH1 3LE Durham, UK
[2]Department of Biochemistry and Systems Biology, University of Liverpool, Crown Street, L69 7ZB Liverpool, UK

[*]Corresponding author's e-mail address: nsavage@liverpool.ac.uk

Citation: Bagdassarian KS, Etchells JP, Savage NS. 2023. A mathematical model integrates diverging PXY and MP interactions in cambium development. *In Silico Plants*. **2023**: diad003; doi: 10.1093/insilicoplants/diad003

Handling Editor: Amy Marshall-Colon

ABSTRACT

The cambium is a secondary meristematic tissue in plant stems, roots and hypocotyls. Here, cell divisions occur that are required for radial growth. In most species that undergo secondary growth, daughters of cell divisions within the cambium differentiate into woody xylem cells towards the inside of the stem, or phloem towards the outside. As such, a pattern of xylem-cambium-phloem is present along the radial axis of all secondary vascular tissues, whether in stem, hypocotyl or root. A ligand-receptor tracheary element, trans-differentiation inhibitory factor (TDIF)-PHLOEM INTERCALATED WITH XYLEM (PXY) promotes cell division in the cambium, as do the phytohormones, cytokinin and auxin. An auxin response factor, MONOPTEROS (MP), has been proposed to initiate cambial cell divisions by promoting PXY expression, however, MP has also been reported to repress cambial cell divisions later in development where TDIF-PXY complexes are also reported to suppress MP activity. Here, we used a mathematical modelling approach to investigate how MP cell division-promoting activity and cell division-repressing activity might be integrated into the same network as a negative feedback loop. In our model, this feedback loop improved the ability of the cambium to pattern correctly and was found to be required for normal patterning as the stability of MP was increased. The implications of this model in early and late cambium development are discussed.

KEYWORDS: Cambium; development; mathematical modelling; phloem; signalling; xylem.

1. INTRODUCTION

Most terrestrial plant biomass is derived from the cambium, which promotes radial, secondary growth of stems in gymnosperms and woody angiosperms. The cambium constitutes a bifacial meristem from which phloem and xylem tissues are derived. As stem cells in the cambium divide, their daughters differentiate into phloem towards the outside of the stem, or xylem towards the inside (Esau 1960, 1965; Evert 2006). The cambium represents an atypical stem cell population by virtue of its bifacial nature, but also because it arises post-embryonically, forming de novo following germination (Baum *et al.* 2002). As such, cambial stem cells are defined within a pre-patterned tissue that arises during embryogenesis (Scheres *et al.* 1994; De Rybel *et al.* 2014). In Arabidopsis roots the pre-pattern constitutes a central file of xylem cells with phloem poles on either side (Fig. 1A). Each phloem pole is separated from the central xylem by a row of procambium cells (Dolan *et al.* 1993). Formation of the cambium at the initiation of secondary growth occurs when the cells of xylem identity act as 'organiser cells', promoting their neighbours to form the cambial meristem and divide (Smetana *et al.* 2019). This marks the transition from primary to secondary growth.

In Arabidopsis, the events that promote the transition from primary to secondary growth start with the formation of an auxin maximum in the organizer cells which have xylem identity (Smetana *et al.* 2019). Auxin responses are mediated by transcription factors in the auxin response factor (ARF) family (Roosjen *et al.* 2018), and the auxin maximum in the organiser cells results in activation of MONOPTEROS (MP; also known as ARF5) (Smetana *et al.* 2019). MP promotes the expression of auxin efflux carriers, members of the PIN family (Przemeck *et al.* 1996; Hardtke and Berleth 1998; Bhatia *et al.* 2016; Brackmann *et al.* 2018). Thus, auxin promotes its own movement via an

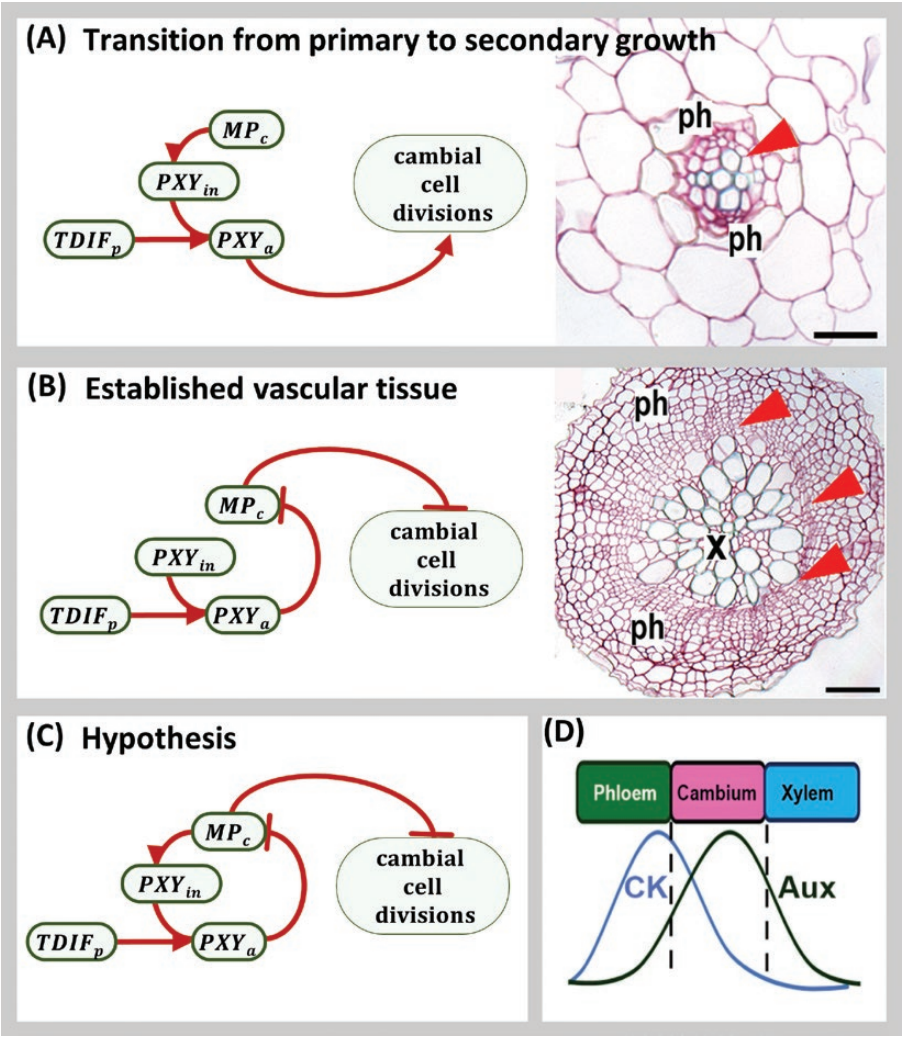

Figure 1. Diagrams showing interactions between PXY and MP in Arabidopsis secondary growth, and tissue morphology in which these interactions occur. (A) MP at the top of a feed-forward loop which promotes cambial cell divisions. MP activates PXY expression (PXY_{in}), and PXY promotes initial cambial cell divisions upon interaction with TDIF (PXY_a). Image on the right shows a root transverse section with initial cambial cell division. (B) MP acts as a repressor of cambium cell division in established vascular tissue. When secondary growth is established, MP represses cambial cell division and is repressed by TDIF-PXY (PXY_a). Image shows root with an established cambium. (C) Hypothesised MP negative feedback loop. Combination of network diagrams in (A) and (B). TDIF-PXY (PXY_a) promotes cambial cell division via the prevention of MP activation. (D) Schematic showing an auxin (Aux) maxima on the xylem side of the cambium and cytokinin (CK) concentration highest in the phloem (adapted from (Fischer *et al.* 2019)). Scale bars are 20 μm (A), or 50 μm (B). X is xylem, ph is phloem, red arrowheads point to dividing cambial cells.

auxin, MP, PIN pathway. Auxin, acting through MP, also activates the expression of members of the Class III homeodomain leucine-zipper (HD-Zip-III) family of transcription factors and PHLOEM INTERCALATED WITH XYLEM (PXY) receptor kinase (Baima *et al.* 1995; Mattsson *et al.* 2003; Ohashi-Ito and Fukuda 2003; Izhaki and Bowman 2007; Zhou *et al.* 2007; Donner *et al.* 2009; Carlsbecker *et al.* 2010; Ursache *et al.* 2014; Smetana *et al.* 2019). PXY expression is promoted by HD-Zip-III transcription factors (Smetana *et al.* 2019), thus MP sits at the top of a feed-forward loop in which MP activates HD-Zip-III's, and both MP and HD-Zip-III's promote PXY expression. Activation of PXY expression promotes the first cell divisions of the cambium (Fig. 1A) (Smetana *et al.* 2019).

PXY is a central regulator of vascular proliferation in plant vascular tissue (Hirakawa *et al.* 2008; Etchells and Turner 2010). In Arabidopsis, its cognate ligand, tracheary element differentiation inhibitory factor (TDIF), is a dodecapeptide derived from two genes, CLE41 and CLE44 that are expressed in the phloem (Ito *et al.* 2006). TDIF-PXY complexes are in an active state and promote cell divisions, both by excluding xylem differentiation from the cambium stem cells and by promoting the divisions themselves (Hirakawa *et al.* 2008; Etchells and Turner 2010). BES1, a transcription factor that promotes xylem activity is degraded upon TDIF-PXY binding, thus preventing premature xylem differentiation (Kondo *et al.* 2014). TDIF-PXY signalling promotes cell division by activating the expression of homeodomain transcription factors WOX4 and WOX14 (Hirakawa *et al.* 2010; Etchells *et al.* 2013; Smit *et al.* 2020).

Cytokinin (CK) is another hormone that plays an important role in PIN regulation (Pernisová *et al.* 2009; Růžička *et al.*

2009; Bishopp *et al.* 2011a; Marhavý *et al.* 2014; Šimášková *et al.* 2015), cambium formation, and subsequent cambium cell divisions (Matsumoto-Kitano *et al.* 2008; Hejátko *et al.* 2009; Ye *et al.* 2021). Indeed, mutants lacking CK biosynthesis never form a cambium (Matsumoto-Kitano *et al.* 2008). Antagonistic relationships between auxin and CK feature in pattern formation across plant vascular tissue (Schaller *et al.* 2015). Auxin signalling induces ARABIDOPSIS HISTIDINE PHOSPHOTRANSFER PROTEIN 6, a pseudophosphotransfer protein which acts to dampen CK signalling (Suzuki *et al.* 1998; Mähönen *et al.* 2006; Werner *et al.* 2006; Moreira *et al.* 2013). Thus, in cells with an auxin maximum, such as those of xylem identity during primary growth, CK signalling is attenuated (Suzuki *et al.* 1998; Mähönen *et al.* 2006; Matsumoto-Kitano *et al.* 2008; Moreira *et al.* 2013). In turn, CK suppresses auxin active transport through decreasing the PIN levels at the post-transcriptional stage (Ioio *et al.* 2008; Pernisová *et al.* 2009; Bishopp *et al.* 2011b; Marhavý *et al.* 2011; Zhang *et al.* 2011; Šimášková *et al.* 2015). CK is bulk-transported down the phloem (Hirose *et al.* 2008; Bishopp *et al.* 2011b), reinforcing the pattern of maximal CK signalling in the phloem, and minimal in the xylem (Uggla *et al.* 1996; Tuominen *et al.* 1997; Uggla *et al.* 1998; Immanen *et al.* 2016; Smetana *et al.* 2019). These observations are supported by the visualisation of a TCSn CK response marker, which unambiguously shows greater expression in phloem than xylem in Arabidopsis roots undergoing secondary growth (Ye *et al.* 2021). Secondary vascular tissues are thus characterised by CK on the phloem side of the cambium, and an auxin maximum in the cambium cells adjacent to the xylem (Uggla *et al.* 1996, 1998; Tuominen *et al.* 1997; Immanen *et al.* 2016; Smetana *et al.* 2019)(Fig. 1D), which is the tissue in which PXY is expressed (Fisher and Turner 2007).

As discussed above, during the transition from primary to secondary growth MP is at the top of a feed-forward loop which promotes cambial cell divisions (Fig. 1A). By contrast MP has been reported to act as a repressor of cambium cell division in established vascular tissue (Fig. 1B). *mp* mutants demonstrate increases in the size of cambium-derived tissues, and high MP levels were found to reduce cambial-derived tissue (Brackmann *et al.* 2018). Thus, the data suggest that the influence of MP on cambial cell divisions changes during development: MP promotes cambium cell division in initiating vascular tissue (Smetana *et al.* 2019, Fig. 1A), but MP represses cambium cell divisions in established vascular tissue (Brackmann *et al.* 2018, Fig. 1B). During the later stages of development, TDIF-PXY was shown to represses MP activity by preventing phosphorylation at a site that contributes to MP's activation (Han *et al.* 2018, Fig. 1B).

When considering the Arabidopsis data in the form of network diagrams the seemingly contradictory data, where MP acts as a promoter (Fig. 1A) and repressor of cambial divisions (Fig. 1B), are not contradictory at all. Rather, collectively, they support the hypothesis whereby MP directly represses cambial cell divisions (Brackmann *et al.* 2018) and MP promotes the activation of PXY, active PXY then promotes cambial cell divisions (Smetana *et al.* 2019) via the prevention of MP activation (Han *et al.* 2018). As such these interactions constitute an MP negative feedback loop (Fig. 1C), whereby MP promotes its own down-regulation; MP promotion of PXY, and PXY suppression of MP. The hypothesised MP negative feedback loop was tested using mathematical modelling. The model was built using the cellular organisation present in the Arabidopsis initiating cambium, just after the transition into secondary growth (Fig. 1A). It was posited that if the MP feedback loop was indeed present in this tissue (i.e. addition of feedback to the network in Fig. 1A to produce the network in Fig. 1C), then its presence would improve the ability of the cambium to maintain CK and auxin concentration profiles (Fig. 1D) (Uggla *et al.* 1996; Tuominen *et al.* 1997; Uggla *et al.* 1998; Immanen *et al.* 2016; Smetana *et al.* 2019; Fu *et al.* 2021). Including MP negative feedback did improve the ability of the modelled tissue to pattern correctly and furthermore, the addition of MP negative feedback never hindered the modelled tissues' ability to pattern correctly. Interestingly, when the stability of MP was increased by reducing its basal degradation rate, MP negative feedback was required for the modelled tissue to pattern correctly. One explanation of these findings is that the MP-PXY-MP feedback loop is present both in initiating and established cambium. Other factors, such as differences in tissue topology, or molecular actors, may then influence the feedback loop to favour MP activation of PXY early in development, but PXY repression of MP in established tissue, interesting avenues for future study.

2. MATERIALS AND METHODS

2.1 Model formulation

A one-dimensional reaction-diffusion model was built to investigate the consequence of MP negative feedback on vascular tissue patterning. The model contained three, well-mixed, spatial domains; the phloem, cambium and xylem. The lengths of the domains were set to; 2.6 μm for the phloem, 1.2 μm for the cambium and 10.8 μm for the xylem, which were derived from previously described *in planta* measurements (Wang *et al.* 2019). The model contained components which have been shown to impact vascular tissue patterning. Namely, the hormones CK and auxin, the PIN proteins, the activator of PIN proteins MP, the receptor-kinase PXY and its ligand TDIF.

Both hormones, CK and auxin, move between the modelled spatial domains. CK was the only component of the model which moved between the domains via diffusion. CK is rapidly transported down the phloem from the shoot to the root (Hirose *et al.* 2008) and is thus modelled as a constant CK source. CK diffuses between the phloem and the cambium. CK moving back into the phloem from the cambium is subsumed by the shoot-to-root flow. CK also diffuses between the cambium and xylem. Once in the xylem, CK diffusing from the xylem to the central tissues, rather than back into the cambium, is lost as there is no data to suggest that CK re-enters the xylem during secondary growth. The diffusion coefficient of CK was set to 220 $\mu m^2/s$ (Moore *et al.* 2015). The phloem was modelled to be a constant source of auxin as that too is transported down the phloem (Goldsmith 1977; Swarup *et al.* 2001; Friml *et al.* 2002; Friml *et al.* 2002; Blakeslee *et al.* 2005; Blilou *et al.* 2005; Kepinski and Leyser 2005; Ljung *et al.* 2005; Vieten *et al.* 2005; Michniewicz *et al.* 2007; Adamowski and Friml 2015; Zhou and Luo 2018). However, as auxin moves between cells via PINs, auxin movement was described as a reaction in the model. Any hormone moving from the cambium back into the phloem was considered to be transported out via bulk transport (Michniewicz *et*

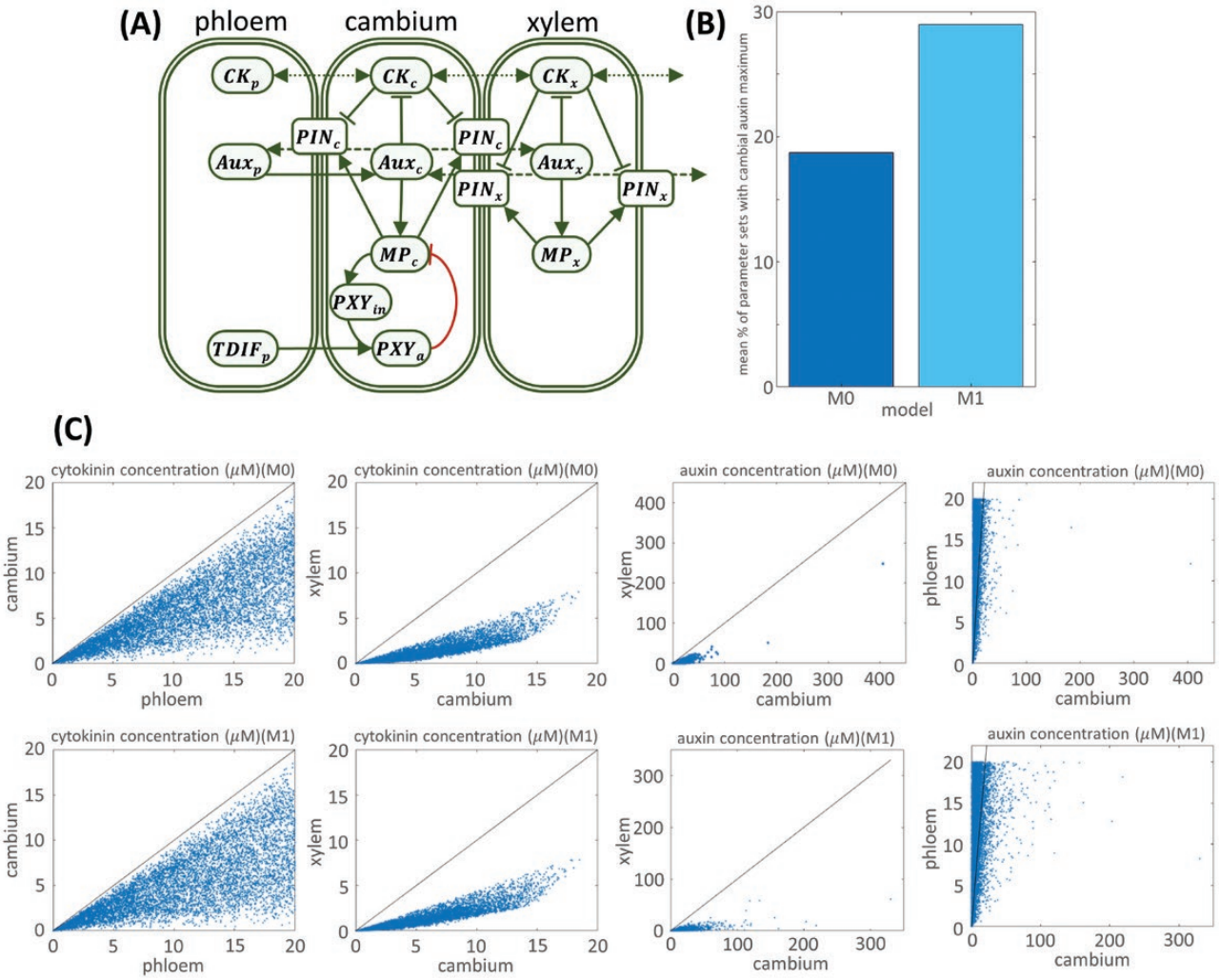

Figure 2. Modelled interactions and numerical results. (A) Diagram showing modelled interactions. Links represent interactions. Arrows represent promotion, barbed ended links represent repression. The dotted arrows show CK diffusion. The dashed arrows show auxin movement via the PIN proteins. Red link highlights the hypothesised MP negative feedback. (B) The mean percentage of parameter sets that achieve cambium auxin maximum in the presence (M1) or absence (M0) of MP negative feedback. Mean calculated from 15 repeat experiments, each containing 500 parameter sets. *P*-value = 2×10^{-14} calculated using Welch's two-sample t-test. (C) Concentration comparisons of the hormones cytokinin and auxin within different tissues. A total of 7500 data points in each graph. Each data point is the steady-state solution for an individual parameter set. Black line represents the boundary when concentrations are equal.

al. 2007; Hirose *et al.* 2008; Bishopp *et al.* 2011b; Adamowski and Friml 2015), leaving the phloem hormone concentration constant. Any hormone moving from the xylem on the opposing side to the cambium was removed from the model.

PXY's peptide ligand, TDIF, is cleaved from CLE41 and CLE44 peptides which are transcribed and translated in the phloem. Following excretion from phloem cells, TDIF moves to the cambium (Ito *et al.* 2006; Hirakawa *et al.* 2008; Etchells and Turner 2010). As TDIF is continuously produced in the phloem, the concentration of TDIF is modelled as a constant (Ito *et al.* 2006; Hirakawa *et al.* 2008; Etchells and Turner 2010).

Reactions included in the model were; the suppression of CK by auxin (Nordström *et al.* 2004; Mähönen *et al.* 2006; Werner *et al.* 2006; Müller and Sheen 2008; Bishopp *et al.* 2011a; Moreira *et al.* 2013), the release of MP inhibition by auxin (Chen *et al.* 2015), the suppression of PINs by CK (Ioio *et al.* 2008; Müller and Sheen 2008; Pernisová *et al.* 2009; Růžička *et al.* 2009; Bishopp *et al.* 2011b; Šimášková *et al.* 2015), the activation of PINs by MP (Przemeck *et al.* 1996; Hardtke and Berleth 1998; Bhatia *et al.* 2016; Krogan *et al.* 2016), the induction of PXY transcription by MP, the activation of PXY by TDIF (Ito *et al.* 2006; Fisher and Turner 2007; Hirakawa *et al.* 2008; Etchells and Turner 2010), and the repression of MP by activated PXY (Han *et al.* 2018). Transcription and translation were not separated in the model and were modelled as one reaction. Reactions were modelled using mass action kinetics. The reactions included in the model are illustrated in Fig. 2A and summarised in Table 1.

Equations (1)–(10) describe the model. $[AUX_p]$, $[AUX_c]$ and $[AUX_x]$ denote the concentrations of auxin in the phloem, cambium and xylem, respectively. The concentration of PINs and MP in the cambium and xylem are denoted, $[PIN_c]$, $[MP_c]$ and $[PIN_x]$, $[MP_x]$, respectively. The concentration of TDIF in the phloem is denoted, $[TDIF_p]$. The concentration of inactive PXY (not bound to TDIF) and active PXY (TDIF-PXY) in the cambium

Table 1. Modelled reactions and diffusion. Table describing the reactions included in the model, their references, their reaction number and units. Basal degradation is not shown in the table but has been modelled for all components. Basal degradation is denoted d_*, where $*$ is the component's name.

Reaction number	Reaction units	Reaction description	Reference
r_1	s^{-1}	Auxin flux from the phloem to the cambium	(Swarup *et al.* 2001; Friml *et al.* 2002; Friml *et al.* 2002; Blakeslee *et al.* 2005; Blilou *et al.* 2005)
r_2	$\mu M^{-1}s^{-1}$	Auxin transport via PINs	(Goldsmith 1977; Blakeslee *et al.* 2005; Blilou *et al.* 2005; Vieten *et al.* 2005)
r_3	$\mu M^{-1}s^{-1}$	Auxin suppression of cytokinin	(Nordström *et al.* 2004; Mähönen *et al.* 2006; Werner *et al.* 2006; Müller and Sheen 2008; Bishopp *et al.* 2011a; Moreira *et al.* 2013)
r_4	s^{-1}	Auxin-induced release of MP	(Ulmasov *et al.* 1997, 1999; Dharmasiri *et al.* 2005; Peer 2013; Chen *et al.* 2015; Weijers and Wagner 2016)
r_5	$\mu M^{-1}s^{-1}$	Cytokinin suppression of pins	(Ioio *et al.* 2008; Müller and Sheen 2008; Pernisová *et al.* 2009; Růžička *et al.* 2009; Bishopp *et al.* 2011b; Šimášková *et al.* 2015)
r_6	s^{-1}	MP activation of PINs	(Przemeck *et al.* 1996; Hardtke and Berleth 1998; Bhatia *et al.* 2016; Krogan *et al.* 2016)
r_7	s^{-1}	MP induces PXY transcription	(Smetana *et al.* 2019)
r_8	$\mu M^{-1}s^{-1}$	TDIF activates PXY	(Ito *et al.* 2006; Fisher and Turner 2007; Hirakawa *et al.* 2008; Etchells and Turner 2010)
r_9	$\mu M^{-1}s^{-1}$	Active PXY repression of monopteros	(Han *et al.* 2018)
D_{CK}	$\mu m^2 s^{-1}$	Cytokinin diffusion	(Hirose *et al.* 2008)

are denoted, $[PXY_{in}]$ and $[PXY_a]$, respectively. d_* denotes the rate of basal degradation of the component $*$. r_i denotes the reaction rate of reaction i. The concentration of CK in the phloem, cambium and xylem are denoted, $[CK_p]$, $[CK_c]$ and $[CK_x]$, respectively. CK moves between tissues via diffusion. D_{CK} denotes the diffusion coefficient of CK. As the concentration $[CK_p]$ is a constant and CK moving from the phloem to central tissues is lost, CK movement is not described by the Laplacian operator. Let $\tilde{\nabla}()$ denote the function describing the diffusive movement of CK across the tissues. The explicit definition of $\tilde{\nabla}()$ can be found in the Supporting Information in the form of the finite difference scheme used to calculate the changes in CK concentration resulting from diffusion, $D_{CK}\ \tilde{\nabla}()$. Changes in concentrations due to reaction dynamics, for all modelled components, were calculated using Euler's method. The initial concentrations for components whose dynamics were described by equations (1)–(10) were zero, for all numerical solutions.

In order to investigate the hypothesis that MP negative feedback could improve the ability of the modelled tissue to pattern auxin and CK correctly (Fig. 1D), the model was solved and analysed, with and without MP negative feedback. The model with MP negative feedback was described by equations (1)–(10) with all parameter values greater than zero. The model without MP negative feedback was also described by equations (1)–(10) but with a number of parameters set to zero. r_9 is the rate at which active PXY represses MP (red link Figs. 1B, C, 2A) as this reaction does not exist in the model without MP negative feedback r_9 was set to zero. With $r_9 = 0$ the parameters $[TDIF_p]$, r_7, r_8, $d_{PXY_{in}}$ and d_{PXY_a} have no effect on the auxin and CK concentrations as they are downstream of MP (Figs. 1A and 2A). Thus, in the model without MP negative feedback parameters $[TDIF_p]$, r_7, r_8, $d_{PXY_{in}}$ and d_{PXY_a} were also set to zero. All numerical solutions presented in the Results section, and all codes used to solve and analyse the numerical solutions, can be found on GitHub (Bagdassarian 2021c, 2021a, 2021b). Steady-state analysis can be found in the Results section and the Supporting Information.

$$\frac{d}{dt}[Aux_c] = r_1[Aux_p] + \frac{r_2}{2}[PIN_x][Aux_x] - r_2[Aux_c][PIN_c] - d_{Aux}[Aux_c] \quad (1)$$

$$\frac{d}{dt}[Aux_x] = \frac{r_2}{2}[PIN_c][Aux_c] - r_2[Aux_x][PIN_x] - d_{Aux}[Aux_x] \quad (2)$$

$$\frac{\partial}{\partial t}[CK_c] = D_{CK}\ \tilde{\nabla}\left([CK_p], [CK_c], [CK_x]\right) - r_3[Aux_c][CK_c] - d_{CK}[CK_c] \quad (3)$$

$$\frac{\partial}{\partial t}[CK_x] = D_{CK}\ \tilde{\nabla}([CK_c], [CK_x]) - r_3[Aux_x][CK_x] - d_{CK}[CK_x] \quad (4)$$

$$\frac{d}{dt}[MP_c] = r_4[Aux_c] - r_9[PXY_a][MP_c] - d_{MP}[MP_c] \quad (5)$$

$$\frac{d}{dt}[MP_x] = r_4[Aux_x] - d_{MP}[MP_x] \quad (6)$$

$$\frac{d}{dt}[PIN_c] = r_6[MP_c] - r_5[CK_c][PIN_c] - d_{PIN}[PIN_c] \quad (7)$$

$$\frac{d}{dt}[PIN_x] = r_6[MP_x] - r_5[CK_x][PIN_x] - d_{PIN}[PIN_x] \quad (8)$$

$$\frac{d}{dt}[PXY_{in}] = r_7[MP_c] - r_8[PXY_{in}][TDIF_p] - d_{PXY_{in}}[PXY_{in}] \quad (9)$$

$$\frac{d}{dt}[PXY_a] = r_8[PXY_{in}][TDIF_p] - d_{PXY_a}[PXY_a] \quad (10)$$

2.2 Plant tissue section preparation

Arabidopsis plants were grown for 14 days on MS media without sucrose, or on potting compost for 30 days. In both cases, the upper 0.5 cm of the root adjacent to the hypocotyl was taken for imaging the cambium. For imaging, plants were fixed in a formalin-acetic-alcohol solution and dehydrated through an ethanol series. Samples were infiltrated and embedded in JB4 (polysciences) according to the manufacturer's instructions. 4 μm sections were taken using a glass blade on a rotary microtome prior to transfer to microscope slides. Sections were stained for 30 s in 0.05% aqueous toluidine blue (14-day samples), or in 0.05% aqueous ruthenium red for 10 s, then toluidine blue for 10 seconds (30-day samples). Sections were mounted in histomount prior to visualisation on a Zeiss Axioskop.

3. RESULTS

For each of the models, with and without MP negative feedback, 7500 parameter sets were chosen at random from the arbitrary interval $(0, 20]$. A steady-state solution was obtained numerically (Methods). The steady state solutions where then compared to the observed concentration profiles of CK and auxin in the root (Fig. 1D). Steady-state solutions were used because while the absolute levels of the hormone in each tissue may fluctuate, CK concentration is greatest in the phloem and least in the xylem, and auxin concentration is greatest in the cambium throughout the developmental stage being modelled (Fischer *et al.* 2019). Note, the spatial domains within the model are well mixed giving one concentration of hormone for each tissue. A match between steady-state solution and data was defined as a CK maximum in the phloem and minimum in the xylem, and an auxin maximum in the cambium. Statistical analysis was performed on the numerical data by sampling the 7500 solutions for each model.

As numerical solutions sample small areas of parameter space steady-state analysis was also performed. Relationships derived using steady-state analysis were verified numerically using the numerical solutions.

3.1 Numerical solutions suggest that MP negative feedback improves the ability of the modelled root to achieve a cambial auxin maximum

As the CK concentration profile did not distinguish between models with and without MP negative feedback, the ability of MP negative feedback to improve the observed auxin maximum in the cambial tissue was tested (Fig. 1D). In the model without MP negative feedback (referred to as model M0), 1406 parameter sets (18.75%) had a cambial auxin maximum at steady state, compared to 2172 parameter sets (28.96%) for the model with MP negative feedback (referred to as model M1). To calculate the statistical significance of these results, the data for models M0 and M1 were divided up to produce repeat experiments. Figure 2B shows the mean percentage of parameter sets which achieved a cambial auxin maximum for the data divided into 15 repeat experiments, each containing 500 parameter sets. The mean percentages for the divided data were 18.75% for model M0 and 28.96% for model M1. The normal distribution of the percentage data was confirmed using the Shapiro–Wilk test. Welch's two-sample *t*-test was performed on the percentage data, giving a *P*-value of 2×10^{-14}. Statistical analysis on the data divided in numerous ways can be found in the Supplement. For all data divisions tested, the *P*-values were less than 0.05, indicating the difference between the data produced by models with and without MP negative feedback was significantly different. Thus the inclusion of MP negative feedback significantly increased the ability of the model to reproduce observed biological data by 10.21% (Fig. 2B).

3.2 Auxin concentrations in the cambium and phloem determine whether or not the models reproduce the biological data

To understand how the models which did not reproduce biological data differed from the biological data the steady-state concentrations were investigated further. The CK concentration profile was considered first. For all of the 15,000 parameter sets, 7500 for each model, the concentration of CK in the phloem, $[CK_p]$, was greater than the concentration of CK in the cambium, $[CK_c]$ (Fig. 2C), and the concentration of CK in the cambium was greater than the concentration of CK in the xylem, $[CK_x]$ (Fig. 2C). Thus, both models, with and without MP negative feedback, reproduced the CK concentration profile observed *in planta*. Analysis on the numerical scheme used to solve the models confirmed that the steady-state concentration of CK would always be greatest in the phloem and least in the xylem (Supporting Information). The result held for all CK diffusion coefficients and reaction rates greater than zero. Furthermore, the result held if the reaction rates and diffusion coefficients were different in each tissue.

The ability of the models to reproduce the CK concentration profile observed in plants is unsurprising. CK movement is modelled by diffusion (Hirose *et al.* 2008). The phloem contains the only source of CK within the models. CK diffuses from the phloem through the cambium and xylem tissues (Fig. 2A). Thus, the only way for CK to be present in the cambium or xylem is via diffusive movement. As such, the concentration of CK in the cambium will be lower than the concentration of CK in the phloem, and the concentration of CK in the xylem will be lower than the concentration of CK in the cambium. There is one reaction affecting the concentrations of CK in the cambium and xylem, the suppression of CK by auxin. Here, auxin negatively regulates CK concentration and signalling (Nordström *et al.* 2004; Mähönen *et al.* 2006; Werner *et al.* 2006; Müller and Sheen 2008; Bishopp *et al.* 2011a; Moreira *et al.* 2013). The suppression of CK by auxin acts to reduce the concentrations of active CK in the cambium and xylem. Therefore, it would be possible for there to be a transient phase in which auxin in the cambium suppressed cambial CK to produce a CK concentration which was lower than the xylem CK concentration. However, as CK in the xylem must be replenished from the cambial CK, via diffusion, over time the xylem CK concentration would drop below the concentration of cambial CK.

Next, the steady-state concentrations of auxin were compared. For all 15000 parameter sets the concentration of auxin in the cambium, $[Aux_c]$, was greater than the concentration of auxin in the xylem, $[Aux_x]$ (Fig. 2C). Steady state analysis confirmed that the concentration of auxin in the cambium was always greater than the concentration of auxin in the xylem, for both models (Supporting Information). Thus, the only relationship which determined the ability of the models to reproduce biological data was the comparison of auxin concentrations in the cambium and phloem, $[Aux_p]$ (Fig. 2C).

3.3 Necessary but not sufficient conditions for cambium auxin concentration to be greater than phloem auxin concentration

Using steady state analysis, an inequality was derived which gave a relationship to be satisfied for the auxin concentration in the cambium to be greater than the auxin concentration in the phloem, inequality (11) (Supporting Information). Note that for the model without MP negative feedback $[PXY_a] = r_9 = 0$ giving inequality (12) (Fig. 1, Methods). Thus, the inequalities defining the ability of each model to achieve a cambial auxin maximum differ only by the presence, or not, of MP negative feedback terms, $r_9\,[PXY_a]$.

$$r_1 > \alpha + \beta \frac{1}{(d_{MP} + r_9\,[PXY_a])} \tag{11}$$

$$r_1 > \alpha + \beta \frac{1}{(d_{MP})} \tag{12}$$

Where, $d_{Aux} = \alpha$, and $\left(\frac{r_4 r_6 r_2 [Aux_p]}{2(r_5 [CK_p] + d_{PIN})}\right) = \beta$.

The relationships defining the ability of each model to achieve a cambial auxin maximum were tested numerically. For model M0, all 1406 parameter sets which had a cambial auxin maximum satisfied inequality (12). Similarly, for model M1, all 2172 parameter sets which had a cambial auxin maximum satisfied

inequality (11). For both of the models, all parameter sets which did not satisfy either inequality (11) or (12), did not have a cambial auxin maximum at steady state.

For model M0, 766 parameter sets which did not achieve a cambial auxin maximum satisfied inequality (12). For model M1, 731 parameter sets which did not achieve a cambial auxin maximum satisfied inequality (11). Thus, the relationships given by inequalities (11) and (12) are necessary for the models to achieve a cambial auxin maximum (top row, Table 2), but they are not sufficient to guarantee a cambial auxin maximum (first column, Table 2), i.e. if there is a cambial auxin maximum, the parameters will satisfy inequalities (11) or (12), but inequalities (11) or (12) cannot be used to generate successful parameter sets.

3.4 MP negative feedback always improved the modelled tissues' ability to obtain a cambial auxin maximum

As all parameter sets which achieve a cambial auxin maximum satisfy inequalities (11) or (12), inequalities (11) or (12) were used to ask if MP negative feedback always improved the root's ability to obtain a cambial auxin maximum. If MP negative feedback improves the ability of the root model to achieve a cambial auxin maximum, then two things would be expected to be true. One, the addition of MP negative feedback does not prevent a cambial auxin maximum forming. Two, there should be parameter sets for which MP negative feedback is required for the formation of a cambial auxin maximum. Each of these was addressed in turn.

One, does the addition of MP negative feedback ever prevent a cambial auxin maximum from forming? All parameter values and concentrations are non-negative. Note also, if the concentration of active PXY, $[PXY_a]$, was equal to zero in model M1, then the negative feedback loop in model M1 would be broken (Figs. 1C and 2A, equation (5)). The aim here is to ascertain if MP negative feedback can prevent a cambial auxin maximum from forming, so the negative feedback loop must be present. Thus, for the analysis below, concentrations of active PXY greater than zero were considered. Thus, the down-regulation of MP in the cambium (see equation (5)) is stronger in model M1 than it is in model M0,

$$d_{MP} < d_{MP} + r_9\,[PXY_a] \tag{13}$$

It follows that,

$$\frac{1}{d_{MP}} > \frac{1}{(d_{MP} + r_9\,[PXY_a])} \tag{14}$$

Because all parameter values and concentrations are non-negative α and β are also non-negative. Considering non-trivial values of α and β, which are greater than zero, gives the relationship,

$$\alpha + \beta\frac{1}{d_{MP}} > \alpha + \beta\frac{1}{(d_{MP} + r_9\,[PXY_a])} \tag{15}$$

The left-hand side of inequality (15) is equal to the right-hand side of inequality (12). Thus, if the model without MP negative feedback achieves a cambial auxin maximum, the parameters of that model will satisfy inequality (12) and inequalities (15) and (12) can be combined to get inequality (16).

$$r_1 > \alpha + \beta\frac{1}{d_{MP}} > \alpha + \beta\frac{1}{(d_{MP} + r_9\,[PXY_a])} \tag{16}$$

Inequality (16) states that if model M0 achieves a cambial auxin maximum, then adding MP negative feedback to that model will satisfy inequality (11), and have a cambial auxin maximum.

The analysis states that MP negative feedback does not prevent a cambial auxin maximum forming. This analysis was tested numerically. For model M0, 1406 parameter sets had a cambial auxin maximum at steady state. MP negative feedback was added to these 1406 parameter sets by choosing values, greater than zero, for MP negative feedback parameters ($[TDIF_p]$, r_7, r_8, r_9, $d_{PXY_{in}}$, d_{PXY_a}). Ten sets of MP negative feedback parameters were chosen uniformly at random from the interval $(0, 20]$, for each of the 1406 parameter sets, resulting in 14,060 parameter sets. Model M1 was solved numerically for each of the 14,060 parameter sets. All 14,060 parameter sets achieved a cambial auxin maximum at steady state confirming the analytical results.

Two, are there parameter sets for which MP negative feedback is required for the formation of a cambial auxin maximum? As there are no parameter sets which do not satisfy inequalities (11) or (12) and achieve a cambial auxin maximum (Table 2), parameter sets which do not satisfy inequality (12) will be considered in the following analysis. For MP negative feedback to be required there must be a set of parameters for which the model without MP negative feedback does not achieve a cambial auxin maximum but the model with MP negative feedback does. For model M0, parameter sets which do not satisfy inequality (12) do not obtain a cambial auxin maximum. Those parameters satisfy inequality (17),

Table 2. Analytical relationships necessary but not sufficient. Percentage of 15,000 parameter sets, rounded to two significant figures. 'Y' represents yes. 'N' represents no. Top row: If a parameter set achieves a cambial auxin maximum then it will satisfy ether inequalities (11) or (12). Bottom row: If a parameter set does not achieve a cambial auxin maximum then it may satisfy either inequalities (11) or (12). Left column: If a parameter set satisfies ether inequalities (11) or (12) it may not achieve a cambial auxin maximum. Right column: If a parameter set does not satisfy ether inequalities (11) or (12) it will not achieve a cambial auxin maximum.

		Satisfy inequality 11 or 12	
		Y	**N**
Cambial auxin maximum	**Y**	24%	0
	N	10%	66%

$$\alpha + \beta \frac{1}{(d_{MP})} \geq \mathrm{r}_1 \tag{17}$$

For model M1 to obtain a cambial auxin maximum, the parameters must satisfy inequality (11). Merge inequalities (17) and (11) to get,

$$\alpha + \beta \frac{1}{(d_{MP})} > \alpha + \beta \frac{1}{(d_{MP} + r_9 [PXY_a])} \tag{18}$$

Inequality (18) does not contradict inequality (15), which is always true. Inequality (18) states that there are values of r_9 and $[PXY_a]$ for which model M1 will obtain a cambial auxin maximum, but the cambial auxin maximum would be lost if the MP negative feedback loop were removed, i.e. there are a set of parameters for which MP negative feedback is required to obtain a cambial auxin maximum (Fig. 3). This analysis was tested numerically. There were 2172 parameter sets for model M1 which enabled the model to achieve a cambial auxin maximum. For each of the 2172 parameter sets, the MP negative feedback parameters ($[TDIF_p]$, r_7, r_8, r_9, $d_{PXY_{in}}$, d_{PXY_a}) were set to zero. Model M0 was then solved using the 2172 adjusted parameter sets. 801 of the adjusted parameter sets did not achieve a cambial auxin maximum. Thus, for 10.68% of the 7500 parameter sets chosen at random, from the interval $(0, 20]$, MP negative feedback was required to achieve a cambial auxin maximum. The numerical result confirmed the analysis, that there were areas of parameter space for which model M1 obtained a cambial auxin maximum, but the cambial auxin maximum would be lost if the MP negative feedback loop were removed (Fig. 3).

The analysis and numerical results show that MP negative feedback always improved the model's ability to achieve a cambial auxin maximum, as the addition of MP negative feedback did not prevent a cambial auxin maximum forming and there were parameter sets for which MP negative feedback was required for the formation of a cambial auxin maximum.

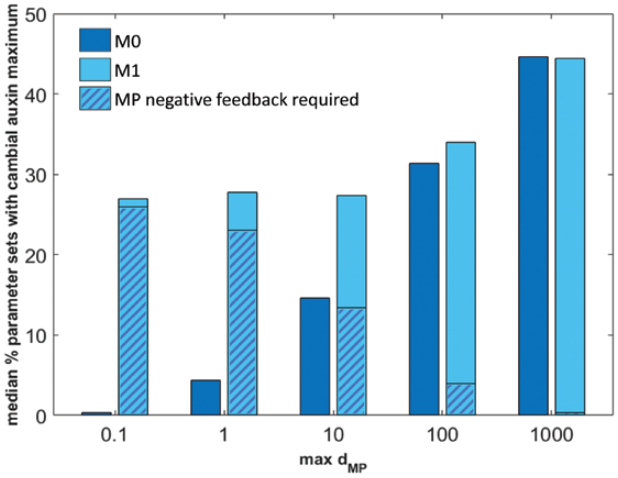

Figure 3. MP negative feedback becomes required as MP becomes more stable. Median percentage of parameter sets that achieve cambium auxin maximum for models M0 and M1. Hashing on M1 data shows the percentage of parameter sets for which MP negative feedback was required. Parameter space for MP degradation is increased by an order of magnitude for each of the 7500 parameter sets. All other parameters were chosen from the interval $(0, 20]$.

3.5 As the stability of MP increases MP negative feedback becomes a requirement for the modelled root to form a cambial auxin maximum

Inequality (18) states that the MP negative feedback loop is required for parameter sets which lie within the space bounded by inequality (18). It was hypothesised that an increase, or decrease, in the size of the space bounded by inequality (18) would increase, or decrease, the number of parameter sets for which the negative feedback loop was required. To find the parameters which had an effect on the size of the space bounded by inequality (18) the distance between the upper and lower bounds, denoted γ, was calculated (equation 19) and rearranged (equation 20).

$$\gamma = \alpha + \beta \frac{1}{d_{MP}} - \left(\alpha + \beta \frac{1}{(d_{MP} + r_9 [PXY_a])}\right) \tag{19}$$

$$\gamma = \beta \frac{1}{d_{MP}} \frac{r_9 [PXY_a]}{(d_{MP} + r_9 [PXY_a])} \tag{20}$$

Equation (20) states that the size of the space bounded by inequality (18), γ, approaches infinity as the basal degradation of MP, d_{MP}, approaches zero, i.e. as MP becomes more stable the number of parameter sets for which MP negative feedback is required would increase. Conversely, γ approaches zero as d_{MP} approaches infinity, as MP becomes more unstable. The hypothesis, that an increase/decrease in γ would lead to an increase/decrease in the number of parameter sets for which the negative feedback loop was required, was tested numerically. All parameters, apart from d_{MP}, were chosen at random from the interval $(0, 20]$, as before. The value of d_{MP} was chosen, at random, from five different intervals, $(0, 1000]$, $(0, 100]$, $(0, 10]$, $(0, 1]$ and $(0, 0.1]$. For each of the d_{MP} intervals, for each of the models, with and without MP negative feedback, 7500 random parameter sets were chosen. First, a steady-state solution was obtained numerically for each parameter set (Methods). Next, to determine the number of parameter sets for which the MP negative feedback loop was required, model M1 parameter sets which obtained a cambial auxin maximum were adjusted to remove the negative feedback loop (i.e. parameters $[TDIF_p]$, r_7, r_8, r_9, $d_{PXY_{in}}$, d_{PXY_a} were set to zero). Model M0 was then solved using the adjusted parameter sets. In order to perform statistical analysis on the steady-state solutions the 7500 parameter sets, for each model, were divided into 15 repeat experiments, each containing 500 parameter sets. The normality of each data set was tested using the Shapiro–Wilk test. Significance measures between two normally distributed data sets were generated using Welch's two-sample *t*-test, otherwise, the Mann–Whitney U test was used (Table 3).

The numerical results confirmed the hypothesis, the percentage of parameter sets for which MP negative feedback was required increased as the upper bound of the interval from

Table 3. MP negative feedback becomes required as MP becomes more stable. Mean and median percentage of parameter sets that achieve cambium auxin maximum for models M0 and M1. 'MP NF required' is the percentage of parameter sets for which MP negative feedback was required. Parameter space for MP degradation is increased by an order of magnitude for each of the 7500 parameter sets. All other parameters were chosen from the interval $(0, 20]$. Normalcy was established using the Shapiro–Wilk test. The *P*-value of the Shapiro–Wilk test is shown, if the *P*-value is greater than 0.05 the distribution is normal. *P*-values less than 2×10^{-16} are shown as 0. The *P*-value of data with a normal distribution has been underlined. Mann–Whitney U test, performed to compare data when one or both data sets were not normal, Welch's two-sample t-test was used otherwise.

15 repeats 500 samples	d_{MP}				
	$(0, 0.1]$	$(0, 1]$	$(0, 10]$	$(0, 100]$	$(0, 1000]$
Mean					
M0	0.53	4.24	14.08	31.03	45.07
M1	26.97	27.44	27.11	33.84	44.28
MP NF required	25.96	22.71	13.69	4.15	0.51
Median					
M0	0.40	4.40	14.60	31.40	44.60
M1	27	27.80	27.40	34	44.40
MP NF required	26	23	13.4	4	0.4
Normal					
M0	0.04	0.94	0.014	0.55	0.64
M1	0.96	0.86	0.54	0.08	0.54
MP NF required	0.68	0.83	0.020	0.81	0.013
Significance comparing M1 and MP NF required					
Mann–Whitney	NA	NA	3×10^{-6}	NA	3×10^{-6}
Welch	0.068	1×10^{-7}	NA	0	NA

which d_{MP} was chosen decreased (Fig. 3, Table 3). Indeed, for the smallest interval of d_{MP} tested, $(0, 0.1]$, there was no significant difference between the percentage of parameter sets which achieved a cambial auxin maximum for model M1 and the percentage of parameter sets for which the MP negative feedback loop was required (Table 3). Thus, as the basal degradation of MP is reduced, MP negative feedback becomes a stronger requirement for the modelled tissue to achieve a cambial auxin maximum.

4. DISCUSSION

4.1 Modelled interactions can replicate hormone patterns in the cambium

Auxin was first observed to influence vascular development in the 1950s via exogenous applications (Torrey 1953). During secondary vascular development, an auxin concentration maximum in the cambium was first observed in pine trees (Uggla *et al.* 1996), a pattern conserved in Arabidopsis (Brackmann *et al.* 2018), the focus species of this study. In Arabidopsis, MP is a key component of the auxin response (Roosjen *et al.* 2018). Recent studies in Arabidopsis have dissected the role of MP in the cambium, both early in development during cambium formation in roots, and later in development in established cambium in the stem. Surprisingly, MP was reported to have opposing functions at these two stages of development. During cambium initiation in seedlings, MP promoted cambial divisions via activation of the PXY receptor kinase (Smetana *et al.* 2019) (Fig. 1A). In established tissue, MP repressed cell division in the cambium, and PXY was found to repress MP activation (Brackmann *et al.* 2018; Han *et al.* 2018; Fig. 1B). One explanation for both MP activities (promotion and repression of cambial cell division) is that MP and PXY form a negative feedback loop (Fig. 1C; addition of PXY repression of MP to Fig. 1A). A mathematical model was generated to understand if MP negative feedback had consequences for the robustness of the system.

The model was characterized by reactions in three domains, phloem, cambium and xylem, with each domain sized to match measured cell sizes in Arabidopsis hypocotyls. None of the parameters in the model had been measured, therefore parameters were sampled from an interval. Model solutions were calculated to steady state. The steady-state solutions were then compared to biological data (Fig. 1D). Steady-state solutions were used because while the absolute levels of the hormone in each tissue may fluctuate, the relationships between the hormone concentrations in different tissues remain unchanged throughout the developmental stage being modelled. The consequences of MP negative feedback were gauged by determining the number of parameter sets in which auxin was correctly patterned, with an auxin maxima in the cambium, in the presence of MP negative feedback, compared to its absence. The modelled CK concentration profile always matched the biological data. The presence of MP negative feedback resulted in a higher proportion of parameter sets generating an auxin maximum in the cambium, 28.96% relative to 18.75% without (Fig. 2B). As such, the inclusion of MP negative feedback increased the ability of the model to reproduce the auxin maxima. Analysis was undertaken which showed that the conclusions drawn using the numerical solutions would be preserved regardless of how the parameters were chosen. Analysis and numerical solutions were then used to provide further support for the MP negative feedback loop. Firstly, for parameter

sets that generated the cambial auxin maxima in the absence of MP negative feedback, the subsequent addition of the feedback loop never disrupted the system such that the auxin maximum was lost. Thus, MP negative feedback did not impede auxin maximum formation in the model. Secondly, for those parameter sets that generated the cambial auxin maximum in the presence of MP negative feedback, for 10.68% of those tested, removal of the MP feedback loop resulted in the loss of the cambium auxin maximum showing that there were areas of parameter space for which MP negative feedback is required. As such, the theoretical evidence described here, supports the notion that the MP negative feedback loop increases the ability of the system to pattern correctly.

4.2 Comparison of models of vascular development

Previously described models have captured elements of vascular development in Arabidopsis. By contrast to the model presented here, most models assess how primary pattern arises in Arabidopsis tissues (Benítez and Hejátko 2013; Cartenì *et al.* 2014; De Rybel *et al.* 2014; Muraro *et al.* 2014; el-Showk *et al.* 2015; Moore *et al.* 2015; Mellor *et al.* 2017). Primary vascular tissue first arises during embryogenesis, with formative divisions occurring at globular and heart stages of Arabidopsis development. De Rybel et al. (2014) generated a mathematical model with four provascular cells to assess how the interplay between auxin, MP and CK, among others might occur (De Rybel *et al.* 2014). This was an important question as at this developmental stage, no phloem exists to deliver CK. During embryogenesis, model performance depended on parameters connected to CK biosynthesis downstream of MP in the xylem axis (De Rybel *et al.* 2014). Comparisons between the model in De Rybel et al. (2014) and the model presented here are challenging as during embryogenesis there is no phloem to transport CK. Nevertheless, interactions such as CK repression of PINs, remain throughout primary development and on into secondary development. Following embryogenesis, the expression of *LOG4*, the CK biosynthesis gene downstream of MP that acts in the embryo persists in the root tip. Here, a CK response reporter, *TCS*, is also active in a *LOG*-dependent manner. During the setup of the primary pattern in the root, the presence of CK is essential in the xylem axis (De Rybel *et al.* 2014; Smet *et al.* 2019; Yang *et al.* 2021). However, shootward from the root tip, *LOG4* expression and xylem *TCS* marker signal are depleted (De Rybel *et al.* 2014). Notably, during secondary growth TCS signal is highest in phloem cells and absent from the xylem (Ye *et al.* 2021). This observation is consistent with the outputs of the model presented here (Fig. 2).

Further differences between primary and secondary growth underly differences between previous vascular development models and the model presented here (Benítez and Hejátko 2013; Cartenì *et al.* 2014; De Rybel *et al.* 2014; Muraro *et al.* 2014; el-Showk *et al.* 2015; Moore *et al.* 2015; Mellor *et al.* 2017). HD-Zip III transcription factors regulate vascular development (Ramachandran *et al.* 2016). Both their action and their negative regulation by microRNAs have been found to maintain a stable bisymmetric pattern using mathematical modelling approaches (Muraro *et al.* 2014). Secondary growth is not characterised by a bisymmetric pattern, but rather by radial symmetry. Furthermore, the site of microRNA production in primary root tissue, the endodermis (Carlsbecker *et al.* 2010), transdifferentiates to periderm during secondary growth (Wunderling *et al.* 2017). The effect on microRNA production through this process is not known. HD-ZIP III genes do have a function downstream of MP in secondary growth. MP acts at the top of a feedforward loop activating both PXY and HD-Zip III. HD-Zip III also promote PXY expression. Consequently, the output of HD-Zip III activation on PXY can be incorporated into MP activation of PXY (Smetana *et al.* 2019). Perhaps the model that bares the most similarity to that presented here is one in which vascular bundle pattern was modelled in Arabidopsis stems (Benítez and Hejátko 2013). This 'dynamic model' by contrast to those described in the primary root, includes TDIF and PXY and is modelled in three domains, xylem, procambium and phloem. It is nevertheless a primary growth model, and interactions between PXY and MP during secondary growth have subsequently been added to the biology literature (Brackmann *et al.* 2018; Smetana *et al.* 2019).

4.3 Auxin acts with receptor kinases to balance stem cell fate

The PXY signalling mechanism is closely related to others that regulate stem cell fate in plant meristems. Among the best characterized of these is the CLAVATA (CLV) system, which regulates the shoot apical meristem. Here CLV3 ligand (related to TDIF), signals to CLV1 (related to PXY) and regulates the expression of *WUSCHEL* (*WUS*), a homeodomain transcription factor (Fletcher *et al.* 1999; Brand *et al.* 2000; Ogawa *et al.* 2008). ChIP-seq data suggests that WUS directly controls the expression of components of auxin transport and response. Auxin is essential at low levels to maintain the shoot apical meristem stems cells (Ma and Li 2019). However, its presence at higher levels is also necessary for organ formation and the flanks of the stem cells in the shoot meristem (Reinhardt *et al.* 2000; Vernoux *et al.* 2000). Thus, the shoot apical meristem represents another system in which the auxin response must be balanced to facilitate differing outcomes, and in this stem cell population, peptide-receptor signalling appears to contribute to balancing these outcomes (Ma and Li 2019). The relationship between auxin and peptide-receptor signalling is likely to be ancient, as in the moss *Physcomitrium*, stem cells are regulated PpRPK2, a PXY/CLV relative, that regulates auxin homeostasis (Nemec-Venza *et al.* 2022).

4.4 Future directions

A striking feature of homeostatic mechanisms in plant meristems, both vascular and apical, is that they must be effective across developmental time. In the case of the cambium, that also must include efficacy across scales. The cambium initiates as cell divisions in xylem adjacent cells, but it can increase in size to multiple cells within a single cell file. While some such variability is present in Arabidopsis, in species such as poplar, in which TDIF-PXY and auxin have both been shown to act in the cambium (Nilsson *et al.* 2008; Etchells *et al.* 2015; Kucukoglu *et al.* 2017; Xu *et al.* 2019), the number of cambium cells fluctuates further, with rapid cambial expansion occurring in early summer prior to cessation of division prior to the onset of winter.

Thus, manipulation of the feedback mechanisms proposed here, possibly by other factors, may influence cambium cell number. These factors could include alterations to feedback caused by differences in tissue topology. For example, high numbers of cambium cells in a cell file (as is seen in established, actively growing cambium) would likely induce changes to CK and auxin gradients due to greater physical distances between the source of hormone and at least a subset of the dividing cells in the cambium. Furthermore, the work here has focussed on the cambium arrangement found in Arabidopsis. Complex vascular arrangements are present in other species, thus it is also an open question as to how the model described here could be adapted to explain such differing morphologies. These include species that form phloem wedges, including members of the *Bignoniaceae* (Pace *et al.* 2009; Spicer and Groover 2010) plants with compound or successive cambia such as species within the *Sapindaceae* (Chery *et al.* 2020) or those with included phloem such as *Heimerliodendron* which form phloem surrounded by cambium on all sides (Studholme and Philipson 1966). The work described here thus acts as a framework to test how the outcomes might differ in two-dimensional space in morphologically accurate tissues at differing stages of cambium development or with differing cambium organisations in future.

Future work also represents an opportunity to refine aspects of the model. For example, one limitation includes the well-mixed assumption. The summative PIN lacking positioning restricts the ability to observe the details of auxin transport under the influence of PXY and MP interactions.

Regarding the perceived change in MP activity throughout development, we hypothesise that other molecular factors have an effect on MP activation of PXY or TDIF-PXY repression of MP to control cambium size during development. It remains an open question for further research, what these factors might be. The requirement for MP negative feedback was high in parameter sets in which basal degradation of MP was reduced (Fig. 3). As such, it might also be interesting to determine MP turnover rates in the vascular cambium at different developmental stages.

ACKNOWLEDGEMENTS

This work was supported by a Biotechnology and Biological Sciences Research Council NLD-DTP studentship.

MODEL AND DATA AVAILABILITY

All numerical solutions presented in the Results section, and all codes used to solve and analyse the numerical solutions, can be found on GitHub (Bagdassarian 2021c, 2021a, 2021b).

SUPPORTING INFORMATION

One file containing the sections, 'Steady state analysis', 'Numerical scheme for cytokinin diffusion', 'Cytokinin concentration profile analysis', 'Statistical analysis of numerical results' and 'Parameter values which achieve a cambial auxin maximum', plus six supporting figures and one supporting table.

CONTRIBUTIONS BY THE AUTHORS

K.S.B. proposed the hypothesis tested within this work, contributed to designing numerical experiments, performed numerical experiments, analysed the numerical data, contributed to the supplemental analysis and gave feedback on the manuscript. J.P.E. supervised the biological aspects of the project and contributed to writing the manuscript. N.S.S. supervised mathematical aspects of the project, designed numerical experiments, performed statistical analysis on numerical data, designed and contributed to the supplemental analysis and contributed to writing the manuscript.

REFERENCES

Adamowski M, Friml J. 2015. PIN-dependent auxin transport: action, regulation, and evolution. *The Plant Cell* 27:20–32. doi:10.1105/tpc.114.134874.

Bagdassarian K, Etchells P, Savage NS. 2021a. *A mathematical model integrates diverging PXY and MP interactions in cambium development: M0 data*, available: github.com/KristineBagdassarian/PXY_MP_model_paper-pt2_no_loop

Bagdassarian K, Etchells P, Savage NS. 2021b. *A mathematical model integrates diverging PXY and MP interactions in cambium development: M1 data*, available: github.com/KristineBagdassarian/PXY_MP_model_paper-pt2_loop

Bagdassarian K, Etchells P, Savage NS. 2021c. *A mathematical model integrates diverging PXY and MP interactions in cambium development: Matlab Solver*, available: github.com/KristineBagdassarian/PXY_MP_model_solver

Baima S, Nobili F, Sessa G, Lucchetti S, Ruberti I, Morelli G. 1995. The expression of the Athb-8 homeobox gene is restricted to provascular cells in *Arabidopsis thaliana*. *Development* 121:4171–4182. doi:10.1242/dev.121.12.4171.

Baum SF, Dubrovsky JG, Rost TL. 2002. Apical organization and maturation of the cortex and vascular cylinder in *Arabidopsis thaliana* (Brassicaceae) roots. *American Journal of Botany* 89:908–920. doi:10.3732/ajb.89.6.908.

Benítez M, Hejátko J. 2013. Dynamics of cell-fate determination and patterning in the vascular bundles of *Arabidopsis thaliana*. *PLoS One* 8(5): e63108. doi:10.1371/journal.pone.0063108.

Bhatia N, Bozorg B, Larsson A, Ohno C, Jönsson H, Heisler MG. 2016. Auxin acts through MONOPTEROS to regulate plant cell polarity and pattern phyllotaxis. *Current Biology* 26:3202–3208. doi:10.1016/j.cub.2016.09.044.

Bishopp A, Help H, El-Showk S, Weijers D, Scheres B, Friml J, Benková E, Mähönen AP, Helariutta Y. 2011a. A mutually inhibitory interaction between auxin and cytokinin specifies vascular pattern in roots. *Current Biology* 21:917–926. doi:10.1016/j.cub.2011.04.017.

Bishopp A, Lehesranta S, Vatén A, Help H, El-Showk S, Scheres B, Helariutta K, Mähönen AP, Sakakibara H, Helariutta Y. 2011b. Phloem-transported cytokinin regulates polar auxin transport and maintains vascular pattern in the root meristem. *Current Biology* 21:927–932. doi:10.1016/j.cub.2011.04.049.

Blakeslee JJ, Peer WA, Murphy AS. 2005. Auxin transport. *Current Opinion in Plant Biology* 8:494–500. doi:10.1016/j.pbi.2005.07.014.

Blilou I, Xu J, Wildwater M, Willemsen V, Paponov I, Friml J, Heidstra R, Aida M, Palme K, Scheres B. 2005. The PIN auxin efflux facilitator network controls growth and patterning in Arabidopsis roots. *Nature* 433:39–44. doi:10.1038/nature03184.

Brackmann K, Qi J, Gebert M, Jouannet V, Schlamp T, Grünwald K, Wallner ES, Novikova DD, Levitsky VG, Agustí J, Sanchez P, Lohmann JU, Greb T. 2018. Spatial specificity of auxin responses coordinates wood formation. *Nature Communications* 9:1–15. doi:10.1038/s41467-018-03256-2.

Brand U, Fletcher JC, Hobe M, Meyerowitz EM, Simon R. 2000. Dependence of stem cell fate in Arabidopsis on a feedback loop

regulated by CLV3 activity. *Science* 289:617–619. doi:10.1126/science.289.5479.617.
Carlsbecker A, Lee JY, Roberts CJ, Dettmer J, Lehesranta S, Zhou J, Lindgren O, Moreno-Risueno MA, Vatén A, Thitamadee S, Campilho A, Sebastian J, Bowman JL, Helariutta Y, Benfey PN. 2010. Cell signalling by microRNA165/6 directs gene dose-dependent root cell fate. *Nature* 465:316–321. doi:10.1038/nature08977.
Cartenì F, Giannino F, Schweingruber FH, Mazzoleni S. 2014. Modelling the development and arrangement of the primary vascular structure in plants. *Annals of Botany* 114:619–627. doi:10.1093/aob/mcu074.
Chen Q, Liu Y, Maere S, Lee E, Van Isterdael G, Xie Z, Xuan W, Lucas J, Vassileva V, Kitakura S. 2015. A coherent transcriptional feed-forward motif model for mediating auxin-sensitive PIN3 expression during lateral root development. *Nature Communications* 6:1–12. doi:10.1038/ncomms9821.
Chery JG, Pace MR, Acevedo-Rodríguez P, Specht CD, Rothfels CJ. 2020. Modifications during early plant development promote the evolution of nature's most complex woods. *Current Biology* 30:237–244. e2. doi:10.1016/j.cub.2019.11.003.
De Rybel B, Adibi M, Breda AS, Wendrich JR, Smit ME, Novák O, Yamaguchi N, Yoshida S, Van Isterdael G, Palovaara J, Nijsse B, Boekschoten MV, Hooiveld G, Beeckman T, Wagner D, Ljung K, Fleck C, Weijers D. 2014 Integration of growth and patterning during vascular tissue formation in Arabidopsis. *Science* 345(6197):1255215. doi:10.1126/science.1255215.
Dharmasiri N, Dharmasiri S, Estelle M. 2005. The F-box protein TIR1 is an auxin receptor. *Nature* 435:441–445. doi:10.1038/nature03543.
Dolan L, Janmaat K, Willemsen V, Linstead P, Poethig S, Roberts K, Scheres B. 1993. Cellular organisation of the *Arabidopsis thaliana* root. *Development* 119:71–84. doi:10.1242/dev.119.1.71.
Donner TJ, Sherr I, Scarpella E. 2009. Regulation of preprocambial cell state acquisition by auxin signaling in Arabidopsis leaves. *Development* 136:3235–3246. doi:10.1242/dev.037028.
el-Showk S, Blomster T, Siligato R, Marée AF, Mähönen AP, Grieneisen VA. 2015. Parsimonious model of vascular patterning links transverse hormone fluxes to lateral root initiation: auxin leads the way, while cytokinin levels out. *PLoS Computational Biology* 11:e1004450. doi:10.1371/journal.pcbi.1004450.
Esau K. 1960. Anatomy of seed plants. *Soil Science* 90:149.
Esau K. 1965. *Vascular differentiation in plants*. New York: Holt, Rinehart and Winston.
Etchells JP, Mishra LS, Kumar M, Campbell L, Turner SR. 2015. Wood formation in trees is increased by manipulating PXY-regulated cell division. *Current Biology* 25:1050–1055. doi:10.1016/j.cub.2015.02.023.
Etchells JP, Provost CM, Mishra L, Turner SR. 2013. WOX4 and WOX14 act downstream of the PXY receptor kinase to regulate plant vascular proliferation independently of any role in vascular organisation. *Development* 140:2224–2234. doi:10.1242/dev.091314.
Etchells JP, Turner SR. 2010. The PXY-CLE41 receptor ligand pair defines a multifunctional pathway that controls the rate and orientation of vascular cell division. *Development* 137:767–774. doi:10.1242/dev.044941.
Evert RF. 2006. *Esau's plant anatomy: meristems, cells, and tissues of the plant body: their structure, function, and development*. Hoboken, New Jersey: John Wiley & Sons, Inc.
Fischer U, Kucukoglu M, Helariutta Y, Bhalerao RP. 2019. The dynamics of cambial stem cell activity. *Annual Review of Plant Biology* 70:293–319. doi:10.1146/annurev-arplant-050718-100402.
Fisher K, Turner S. 2007. PXY, a receptor-like kinase essential for maintaining polarity during plant vascular-tissue development. *Current Biology* 17:1061–1066. doi:10.1016/j.cub.2007.05.049.
Fletcher JC, Brand U, Running MP, Simon R, Meyerowitz EM. 1999. Signaling of cell fate decisions by CLAVATA3 in Arabidopsis shoot meristems. *Science* 283:1911–1914. doi:10.1126/science.283.5409.1911.
Friml J, Benková E, Blilou I, Wisniewska J, Hamann T, Ljung K, Woody S, Sandberg G, Scheres B, Jürgens G, Palme K. 2002. AtPIN4 mediates sink-driven auxin gradients and root patterning in Arabidopsis. *Cell* 108:661–673. doi:10.1016/S0092-8674(02)00656-6.
Friml J, Wiśniewska J, Benková E, Mendgen K, Palme K. 2002. Lateral relocation of auxin efflux regulator PIN3 mediates tropism in Arabidopsis. *Nature* 415:806–809. doi:10.1038/415806a.
Fu X, Su H, Liu S, Du X, Xu C, Luo K. 2021. Cytokinin signaling localized in phloem noncell-autonomously regulates cambial activity during secondary growth of Populus stems. *New Phytologist* 230:1476–1488. doi:10.1111/nph.17255.
Goldsmith M. 1977. The polar transport of auxin. *Annual Review of Plant Physiology* 28:439–478. doi:10.1146/annurev.pp.28.060177.002255.
Han S, Cho H, Noh J, Qi J, Jung H-J, Nam H, Lee S, Hwang D, Greb T, Hwang I. 2018. BIL1-mediated MP phosphorylation integrates PXY and cytokinin signalling in secondary growth. *Nature Plants* 4:605–614. doi:10.1038/s41477-018-0180-3.
Hardtke CS, Berleth T. 1998. The Arabidopsis gene MONOPTEROS encodes a transcription factor mediating embryo axis formation and vascular development. *The EMBO Journal* 17:1405–1411. doi:10.1093/emboj/17.5.1405.
Hejátko J, Ryu H, Kim G-T, Dobešová R, Choi S, Choi SM, Souček P, Horák J, Pekárová B, Palme K, Brzobohatý B, Hwang I. 2009. The histidine kinases CYTOKININ-INDEPENDENT1 and ARABIDOPSIS HISTIDINE KINASE2 and 3 regulate vascular tissue development in Arabidopsis shoots. *The Plant Cell* 21:2008–2021. doi:10.1105/tpc.109.066696.
Hirakawa Y, Kondo Y, Fukuda H. 2010. TDIF peptide signaling regulates vascular stem cell proliferation via the WOX4 homeobox gene in Arabidopsis. *The Plant Cell* 22:2618–2629. doi:10.1105/tpc.110.076083.
Hirakawa Y, Shinohara H, Kondo Y, Inoue A, Nakanomyo I, Ogawa M, Sawa S, Ohashi-Ito K, Matsubayashi Y, Fukuda H. 2008. Non-cell-autonomous control of vascular stem cell fate by a CLE peptide/receptor system. *Proceedings of the National Academy of Sciences* 105:15208–15213. doi:10.1073/pnas.0808444105.
Hirose N, Takei K, Kuroha T, Kamada-Nobusada T, Hayashi H, Sakakibara H. 2008. Regulation of cytokinin biosynthesis, compartmentalization and translocation. *Journal of Experimental Botany* 59:75–83. doi:10.1093/jxb/erm157.
Immanen J, Nieminen K, Smolander OP, Kojima M, Serra JA, Koskinen P, Zhang J, Elo A, Mähönen AP, Street N, Bhalerao RP, Paulin L, Auvinen P, Sakakibara H, Helariutta Y. 2016. Cytokinin and auxin display distinct but interconnected distribution and signaling profiles to stimulate cambial activity. *Current Biology* 26:1990–1997. doi:10.1016/j.cub.2016.05.053.
Ioio RD, Nakamura K, Moubayidin L, Perilli S, Taniguchi M, Morita MT, Aoyama T, Costantino P, Sabatini S. 2008. A genetic framework for the control of cell division and differentiation in the root meristem. *Science* 322:1380–1384. doi:10.1126/science.1164147.
Ito Y, Nakanomyo I, Motose H, Iwamoto K, Sawa S, Dohmae N, Fukuda H. 2006. Dodeca-CLE peptides as suppressors of plant stem cell differentiation. *Science* 313:842–845. doi:10.1126/science.1128436.
Izhaki A, Bowman JL. 2007. KANADI and class III HD-Zip gene families regulate embryo patterning and modulate auxin flow during embryogenesis in Arabidopsis. *The Plant Cell* 19:495–508. doi:10.1105/tpc.106.047472.
Kepinski S, Leyser O. 2005. Plant development: auxin in loops. *Current Biology* 15:R208–R210. doi:10.1016/j.cub.2005.03.012.
Kondo Y, Tamaki T, Fukuda H. 2014. Regulation of xylem cell fate. *Frontiers in Plant Science* 5. doi:10.3389/fpls.2014.00315.
Krogan NT, Marcos D, Weiner AI, Berleth T. 2016. The auxin response factor MONOPTEROS controls meristem function and organogenesis in both the shoot and root through the direct regulation of PIN genes. *New Phytologist* 212:42–50. doi:10.1111/nph.14107.
Kucukoglu M, Nilsson J, Zheng B, Chaabouni S, Nilsson O. 2017. WUSCHEL-RELATED HOMEOBOX 4 (WOX 4)-like genes regulate cambial cell division activity and secondary growth in Populus trees. *New Phytologist* 215:642–657. doi:10.1111/nph.14631.

Ljung K, Hull AK, Celenza J, Yamada M, Estelle M, Normanly J, Sandberg G. 2005. Sites and regulation of auxin biosynthesis in Arabidopsis roots. *The Plant Cell* 17:1090–1104. doi:10.1105/tpc.104.029272.

Ma L, Li G. 2019. Auxin-dependent cell elongation during the shade avoidance response. *Frontiers in Plant Science* 10. doi:10.3389/fpls.2019.00914.

Mähönen AP, Bishopp A, Higuchi M, Nieminen KM, Kinoshita K, Törmäkangas K, Ikeda Y, Oka A, Kakimoto T, Helariutta Y. 2006. Cytokinin signaling and its inhibitor AHP6 regulate cell fate during vascular development. *Science* 311:94–98. doi:10.1126/science.1118875.

Marhavý P, Bielach A, Abas L, Abuzeineh A, Duclercq J, Tanaka H, Pařezová M, Petrášek J, Friml J, Kleine-Vehn J, Benková E. 2011. Cytokinin modulates endocytic trafficking of PIN1 auxin efflux carrier to control plant organogenesis. *Developmental Cell* 21:796–804. doi:10.1016/j.devcel.2011.08.014.

Marhavý P, Duclercq J, Weller B, Feraru E, Bielach A, Offringa R, Friml J, Schwechheimer C, Murphy A, Benková E. 2014. Cytokinin controls polarity of PIN1-dependent auxin transport during lateral root organogenesis. *Current Biology* 24:1031–1037. doi:10.1016/j.cub.2014.04.002.

Matsumoto-Kitano M, Kusumoto T, Tarkowski P, Kinoshita-Tsujimura K, Václavíková K, Miyawaki K, Kakimoto T. 2008. Cytokinins are central regulators of cambial activity. *Proceedings of the National Academy of Sciences* 105:20027–20031. doi:10.1073/pnas.0805619105.

Mattsson J, Ckurshumova W, Berleth T. 2003. Auxin signaling in Arabidopsis leaf vascular development. *Plant Physiology* 131:1327–1339. doi:10.1104/pp.013623.

Mellor N, Adibi M, El-Showk S, De Rybel B, King J, Mähönen AP, Weijers D, Bishopp A. 2017. Theoretical approaches to understanding root vascular patterning: a consensus between recent models. *Journal of Experimental Botany* 68:5–16. doi:10.1093/jxb/erw410.

Michniewicz M, Brewer PB, Friml J. 2007. Polar auxin transport and asymmetric auxin distribution. *The Arabidopsis Book* 5:e0108.

Moore S, Zhang X, Mudge A, Rowe JH, Topping JF, Liu J, Lindsey K. 2015. Spatiotemporal modelling of hormonal crosstalk explains the level and patterning of hormones and gene expression in *Arabidopsis thaliana* wild-type and mutant roots. *New Phytologist* 207:1110–1122. doi:10.1111/nph.13421.

Moreira S, Bishopp A, Carvalho H, Campilho A. 2013. AHP6 inhibits cytokinin signaling to regulate the orientation of pericycle cell division during lateral root initiation. *PLoS One* 8:e56370. doi:10.1371/journal.pone.0056370.

Müller B, Sheen J. 2008. Cytokinin and auxin interaction in root stem-cell specification during early embryogenesis. *Nature* 453:1094–1097. doi:10.1038/nature06943.

Muraro D, Mellor N, Pound MP, Help H, Lucas M, Chopard J, Byrne HM, Godin C, Hodgman TC, King JR, Pridmore TP, Helariutta Y, Bennett MJ, Bishopp A. 2014. Integration of hormonal signaling networks and mobile microRNAs is required for vascular patterning in Arabidopsis roots. *Proceedings of the National Academy of Sciences* 111:857–862. doi:10.1073/pnas.1221766111.

Nemec-Venza Z, Madden C, Stewart A, Liu W, Novák O, Pěnčík A, Cuming AC, Kamisugi Y, Harrison CJ. 2022. CLAVATA modulates auxin homeostasis and transport to regulate stem cell identity and plant shape in a moss. *New Phytologist* 234:149–163. doi:10.1111/nph.17969.

Nilsson J, Karlberg A, Antti H, Lopez-Vernaza M, Mellerowicz E, Perrot-Rechenmann C, Sandberg G, Bhalerao RP. 2008. Dissecting the molecular basis of the regulation of wood formation by auxin in hybrid aspen. *The Plant Cell* 20:843–855. doi:10.1105/tpc.107.055798.

Nordström A, Tarkowski P, Tarkowska D, Norbaek R, Åstot C, Dolezal K, Sandberg G. 2004. Auxin regulation of cytokinin biosynthesis in *Arabidopsis thaliana*: a factor of potential importance for auxin–cytokinin-regulated development. *Proceedings of the National Academy of Sciences* 101:8039–8044. doi:10.1073/pnas.0402504101.

Ogawa M, Shinohara H, Sakagami Y, Matsubayashi Y. 2008. Arabidopsis CLV3 peptide directly binds CLV1 ectodomain. *Science* 319:294–294. doi:10.1126/science.1150083.

Ohashi-Ito K, Fukuda H. 2003. HD-Zip III homeobox genes that include a novel member, ZeHB-13 (Zinnia)/ATHB-15 (Arabidopsis), are involved in procambium and xylem cell differentiation. *Plant and Cell Physiology* 44:1350–1358. doi:10.1093/pcp/pcg164.

Pace MR, Lohmann LG, Angyalossy V. 2009. The rise and evolution of the cambial variant in Bignonieae (Bignoniaceae). *Evolution & Development* 11:465–479. doi:10.1111/j.1525-142X.2009.00355.x.

Peer WA. 2013. From perception to attenuation: auxin signalling and responses. *Current Opinion in Plant Biology* 16:561–568. doi:10.1016/j.pbi.2013.08.003.

Pernisová M, Klíma P, Horák J, Válková M, Malbeck J, Souček P, Reichman P, Hoyerová K, Dubová J, Friml J, Zažímalová E, Hejátko J. 2009. Cytokinins modulate auxin-induced organogenesis in plants via regulation of the auxin efflux. *Proceedings of the National Academy of Sciences* 106:3609–3614. doi:10.1073/pnas.0811539106.

Przemeck GK, Mattsson J, Hardtke CS, Sung ZR, Berleth T. 1996. Studies on the role of the Arabidopsis gene MONOPTEROS in vascular development and plant cell axialization. *Planta* 200:229–237. doi:10.1007/BF00208313.

Ramachandran P, Carlsbecker A, Etchells JP. 2016. Class III HD-ZIPs govern vascular cell fate: an HD view on patterning and differentiation. *Journal of Experimental Botany* 68:55–69. doi:10.1093/jxb/erw370.

Reinhardt D, Mandel T, Kuhlemeier C. 2000. Auxin regulates the initiation and radial position of plant lateral organs. *The Plant Cell* 12:507–518. doi:10.1105/tpc.12.4.507.

Roosjen M, Paque S, Weijers D. 2018. Auxin response factors: output control in auxin biology. *Journal of Experimental Botany* 69:179–188. doi:10.1093/jxb/erx237.

Růžička K, Šimášková M, Duclercq J, Petrášek J, Zažímalová E, Simon S, Friml J, Van Montagu MC, Benková E. 2009. Cytokinin regulates root meristem activity via modulation of the polar auxin transport. *Proceedings of the National Academy of Sciences* 106:4284–4289. doi:10.1073/pnas.0900060106.

Schaller GE, Bishopp A, Kieber JJ. 2015. The yin-yang of hormones: cytokinin and auxin interactions in plant development. *The Plant Cell* 27:44–63. doi:10.1105/tpc.114.133595.

Scheres B, Wolkenfelt H, Willemsen V, Terlouw M, Lawson E, Dean C, Weisbeek P. 1994. Embryonic origin of the Arabidopsis primary root and root meristem initials. *Development* 120:2475–2487. doi:10.1242/dev.120.9.2475.

Šimášková M, O'Brien JA, Khan M, Van Noorden G, Ötvös K, Vieten A, De Clercq I, Van Haperen JMA, Cuesta C, Hoyerová K, Vanneste S, Marhavý P, Wabnik K, Van Breusegem F, Nowack M, Murphy A, Friml J, Weijers D, Beeckman T, Benková E. 2015. Cytokinin response factors regulate PIN-FORMED auxin transporters. *Nature Communications* 6:8717. doi:10.1038/ncomms9717.

Smet W, Sevilem I, de Luis Balaguer MA, Wybouw B, Mor E, Miyashima S, Blob B, Roszak P, Jacobs TB, Boekschoten M, Hooiveld G, Sozzani R, Helariutta Y, De Rybel B. 2019. DOF2. 1 controls cytokinin-dependent vascular cell proliferation downstream of TMO5/LHW. *Current Biology* 29:520–529.e6. doi:10.1016/j.cub.2018.12.041.

Smetana O, Mäkilä R, Lyu M, Amiryousefi A, Rodriguez FS, Wu M-F, Sole-Gil A, Gavarron ML, Siligato R, Miyashima S, Roszak P, Blomster T, Reed JW, Broholm S, Mähönen AP. 2019. High levels of auxin signalling define the stem-cell organizer of the vascular cambium. *Nature* 565:485–489. doi:10.1038/s41586-018-0837-0.

Smit ME, McGregor SR, Sun H, Gough C, Bågman A-M, Soyars CL, Kroon JT, Gaudinier A, Williams CJ, Yang X, Nimchuk ZL, Weijers D, Turner SR, Brady SM, Etchells JP. 2020. A PXY-mediated transcriptional network integrates signaling mechanisms to control vascular development in arabidopsis. *The Plant Cell* 32:319–335. doi:10.1105/tpc.19.00562.

Spicer R, Groover A. 2010. Evolution of development of vascular cambia and secondary growth. *The New Phytologist* 186:577–592. doi:10.1111/j.1469-8137.2010.03236.x.

Studholme WP, Philipson WR. 1966. Woods with included phloem: Heimer Llodendron Brunonianum and Avicennia Resinifera.

New Zealand Journal of Botany 4:355–365. doi:10.1080/00288825X.1966.10429054.

Suzuki T, Imamura A, Ueguchi C, Mizuno T. 1998. Histidine-containing phosphotransfer (HPt) signal transducers implicated in His-to-Asp phosphorelay in Arabidopsis. *Plant and Cell Physiology* 39:1258–1268. doi:10.1093/oxfordjournals.pcp.a029329.

Swarup R, Friml J, Marchant A, Ljung K, Sandberg G, Palme K, Bennett M. 2001. Localization of the auxin permease AUX1 suggests two functionally distinct hormone transport pathways operate in the Arabidopsis root apex. *Genes & Development* 15:2648–2653. doi:10.1101/gad.210501.

Torrey JG. 1953. The effect of certain metabolic inhibitors on vascular tissue differentiation in isolated pea roots. *American Journal of Botany* 40:525–533. doi:10.2307/2438502.

Tuominen H, Puech L, Fink S, Sundberg B. 1997. A radial concentration gradient of indole-3-acetic acid is related to secondary xylem development in hybrid aspen. *Plant Physiology* 115:577–585. doi:10.1104/pp.115.2.577.

Uggla C, Mellerowicz EJ, Sundberg B. 1998. Indole-3-acetic acid controls cambial growth in Scots pine by positional signaling. *Plant Physiology* 117:113–121. doi:10.1104/pp.117.1.113.

Uggla C, Moritz T, Sandberg G, Sundberg B. 1996. Auxin as a positional signal in pattern formation in plants. *Proceedings of the National Academy of Sciences* 93:9282–9286. doi:10.1073/pnas.93.17.9282.

Ulmasov T, Hagen G, Guilfoyle TJ. 1997. ARF1, a transcription factor that binds to auxin response elements. *Science* 276:1865–1868. doi:10.1126/science.276.5320.1865.

Ulmasov T, Hagen G, Guilfoyle TJ. 1999. Activation and repression of transcription by auxin-response factors. *Proceedings of the National Academy of Sciences* 96:5844–5849. doi:10.1073/pnas.96.10.5844.

Ursache R, Miyashima S, Chen Q, Vatén A, Nakajima K, Carlsbecker A, Zhao Y, Helariutta Y, Dettmer J. 2014. Tryptophan-dependent auxin biosynthesis is required for HD-ZIP III-mediated xylem patterning. *Development* 141:1250–1259. doi:10.1242/dev.103473.

Vernoux T, Kronenberger J, Grandjean O, Laufs P, Traas J. 2000. PIN-FORMED 1 regulates cell fate at the periphery of the shoot apical meristem. *Development* 127:5157–5165. doi:10.1242/dev.127.23.5157.

Vieten A, Vanneste S, Wiśniewska J, Benková E, Benjamins R, Beeckman T, Luschnig C, Friml J. 2005. Functional redundancy of PIN proteins is accompanied by auxin-dependent cross-regulation of PIN expression. *Development* 132:4521–4531. doi:10.1242/dev.02027.

Wang N, Bagdassarian KS, Doherty RE, Kroon JT, Connor KA, Wang XY, Wang W, Jermyn IH, Turner SR, Etchells JP. 2019. Organ-specific genetic interactions between paralogues of the PXY and ER receptor kinases enforce radial patterning in Arabidopsis vascular tissue. *Development* 146:dev177105. doi:10.1242/dev.177105.

Weijers D, Wagner D. 2016. Transcriptional responses to the auxin hormone. *Annual Review of Plant Biology* 67:539–574. doi:10.1146/annurev-arplant-043015-112122.

Werner T, Köllmer I, Bartrina I, Holst K, Schmülling T. 2006. New insights into the biology of cytokinin degradation. *Plant Biology* 8:371–381. doi:10.1055/s-2006-923928.

Wunderling A, Ben Targem M, Barbier de Reuille P, Ragni L. 2017. Novel tools for quantifying secondary growth. *Journal of Experimental Botany* 68:89–95. doi:10.1093/jxb/erw450.

Xu C, Shen Y, He F, Fu X, Yu H, Lu W, Li Y, Li C, Fan D, Wang HC. 2019. Auxin-mediated Aux/IAA-ARF-HB signaling cascade regulates secondary xylem development in Populus. *New Phytologist* 222:752–767. doi:10.1111/nph.15658.

Yang B, Minne M, Brunoni F, Plačková L, Petřík I, Sun Y, Nolf J, Smet W, Verstaen K, Wendrich JR, Eekhout T, Hoyerová K, Van Isterdael G, Haustraete J, Bishopp A, Farcot E, Novák O, Saeys Y, De Rybel B. 2021. Non-cell autonomous and spatiotemporal signalling from a tissue organizer orchestrates root vascular development. *Nature Plants* 7:1485–1494. doi:10.1038/s41477-021-01017-6.

Ye L, Wang X, Lyu M, Siligato R, Eswaran G, Vainio L, Blomster T, Zhang J, Mähönen AP. 2021. Cytokinins initiate secondary growth in the Arabidopsis root through a set of LBD genes. *Current Biology* 31:3365–3373.e7. doi:10.1016/j.cub.2021.05.036.

Zhang W, To JP, Cheng CY, Eric Schaller G, Kieber JJ. 2011. Type-A response regulators are required for proper root apical meristem function through post-transcriptional regulation of PIN auxin efflux carriers. *The Plant Journal* 68:1–10. doi:10.1111/j.1365-313X.2011.04668.x.

Zhou GK, Kubo M, Zhong R, Demura T, Ye ZH. 2007. Overexpression of miR165 affects apical meristem formation, organ polarity establishment and vascular development in Arabidopsis. *Plant and Cell Physiology* 48:391–404. doi:10.1093/pcp/pcm008.

Zhou JJ, Luo J. 2018. The PIN-FORMED auxin efflux carriers in plants. *International Journal of Molecular Sciences* 19:2759. doi:10.3390/ijms19092759.